Interaction with Amyloid β Peptide Compromises the Lipid Binding Function of Apolipoprotein E[†]

Shiori Tamamizu-Kato, Jenny K. Cohen, Carolyn B. Drake, Malathi G. Kosaraju, Jessica Drury, and Vasanthy Narayanaswami*

Center for the Prevention of Obesity, Cardiovascular Disease, and Diabetes, Children's Hospital Oakland Research Institute, 5700 Martin Luther King, Jr. Way, Oakland, California 94609

Received October 17, 2007; Revised Manuscript Received March 6, 2008

ABSTRACT: Apolipoprotein (apo) E is an exchangeable apolipoprotein that plays an integral role in cholesterol transport in the plasma and the brain. It is also associated with protein misfolding or amyloid proteopathy of the β amyloid peptide (Aβ) in Alzheimer's disease (AD) and cerebral amyloid angiopathy. The C-terminal domain (CT) of apoE encompasses two types of amphipathic α helices: a class A helix (residues 216–266) and a class G* helix (residues 273–299). This domain also harbors high-affinity lipoprotein binding and apoE self-association sites that possibly overlap. The objective of this study is to examine if the neurotoxic oligomeric Aβ interacts with apoE CT and if this association affects the lipoprotein binding function of recombinant human apoE CT. Site-specific fluorescence labeling of single cysteine-containing apoE CT variants with donor probes were employed to identify the binding of Aβ bearing an acceptor probe by intermolecular fluorescence resonance energy-transfer analysis. A higher efficiency of energy transfer was noted with probes located in the class A helix than with those located in the class G* helix of apoE CT. In addition, incubation of apoE CT with Aβ severely impaired the lipid binding ability and the overall amount of lipid-associated apoE CT. However, when apoE CT is present in a lipid-bound state, Aβ appears to be localized within the lipid milieu of the lipoprotein particle and not associated with any specific segments of the protein. When our data are taken together, they suggest that Aβ association compromises the fundamental lipoprotein binding function of apoE, which may have implications not only in terms of amyloid buildup but also in terms of the accumulation of cholesterol at extracellular sites.

Apolipoprotein E (apoE)[1] is a 299 residue lipid binding protein that plays an integral role in regulating cholesterol and lipoprotein metabolism in the plasma and the central nervous system (CNS) (*1*). It is comprised of two domains: a 22 kDa N-terminal domain and a 10 kDa C-terminal domain. The two domains are linked by a protease-sensitive loop (*2*). A primary function of apoE is to serve as a ligand for the low-density lipoprotein (LDL) receptor family of proteins, a feature housed predominantly in the N-terminal domain between residues 130 and 150 (*3*). Additionally, the ability to mediate high-affinity binding with lipids and promote cellular cholesterol efflux is an important function of apoE, a feature primarily localized in the C-terminal domain (CT) (*4*). In the brain, a major role for apoE is cholesterol mobilization and delivery from non-neuronal cells, such as the astrocytes, to the neurons, the synaptogenesis activities of which places a steady demand for cholesterol (*5*).

ApoE is considered a prototypical exchangeable apolipoprotein by virtue of its ability to exist in lipid-free and lipid-bound states (*6*). Structurally, apoE is comprised predominantly of amphipathic α helices, whose hydrophobic faces interact with each other in the lipid-free state; in the lipid-bound state, the extensive helix−helix contacts are replaced by helix−lipid contacts. In humans, three major isoforms of apoE have been identified: apoE2, apoE3, and apoE4 (allelic frequency of 0.07, 0.8, and 0.14, respectively). The three isoforms differ only at positions 112 and 158 in the N-terminal domain (NT): Cys/Cys in apoE2, Cys/Arg in apoE3, and Arg/Arg in apoE4. Of these, the ε4 allele of the gene encoding apoE is a major risk factor in developing Alzheimer's disease (AD) and cerebral amyloid angiopathy (CAA). A typical neuropathological feature of both AD and CAA is the presence of misfolded amyloid β peptide (Aβ)

[†] This work was supported by funding from an American Heart Association (AHA) undergraduate (to J.D. and J.K.C.) and Postdoctoral Fellowship (to S.T.-K.), an AHA Grant-in-Aid, Alzheimer's Association Grant (TLL-03-5281), and funds from the Drake Family Trust (to V.N.), 2R01HL064159-06, and National Institutes of Health (NIH) short-term training program to increase diversity in health-related research (HL07807).

* To whom correspondence should be addressed: Children's Hospital Oakland Research Institute, 5700 Martin Luther King, Jr. Way, Oakland CA 94609. Telephone: (510) 428-3885 ext. 2965. Fax: (510) 450-7910. E-mail: vnarayan@chori.org.

[1] Abbreviations: Aβ, amyloid β peptide; AD, Alzheimer's disease; AEDANS, *N*-iodoacetyl-*N*′-(5-sulfo-1-naphthyl)ethylenediamine; apoE, apolipoprotein E; CAA, cerebral amyloid angiopathy; CNS, central nervous system; CT, C-terminal domain; DMPC, dimyristoylphosphatidylcholine; FRET, fluorescence resonance energy transfer; LDL, low-density lipoprotein; MLV, multilamellar vesicle; NT, N-terminal domain; PLC, phospholipase C; TBS, Tris-buffered saline; WT, wild type.

10.1021/bi702097s CCC: $40.75
Published on Web 04/12/2008

(39–42 residues), which accumulates at the extra neuronal sites and in the cerebral microvasculature (*7*).

Aβ is released by the sequential intramembranous proteolytic cleavage of the amyloid precursor protein, an integral protein localized in the neuronal membrane (*8*). The released Aβ tends to oligomerize to form Aβ-derived diffusible ligands or ADDLs and eventually aggregates to form amyloid plaques. The levels of oligomeric Aβ are directly correlated with the cognitive decline, memory loss, and neuronal toxicity noted in AD (*9, 10*). ApoE4 has been associated with AD pathology via different mechanisms (*11*). Interestingly, apoE has been immunolocalized in the amyloid plaques of postmortem brains, forming stable complexes (*12, 13*), possibly because of a direct interaction with Aβ in an apoE-isoform-specific manner. Although several *in vitro* studies demonstrate that Aβ can interact with both lipid-free and lipid-bound forms of apoE (*14–18*), the exact nature of the interaction between the two from a structural viewpoint is not known. Further, the functional consequences of the interaction have been typically attributed to the effect of Aβ on the lipoprotein receptor binding of apoE (*19–22*). However, it should be noted that lipid binding is an essential prerequisite for the receptor binding function of apoE, because it aids in the appropriate presentation of the receptor binding sites to the ligand binding domain of the receptors. The objective of the present study is to evaluate the effect of Aβ association on the lipid or lipoprotein binding function of apoE facilitated by the CT domain.

We employ recombinant human apoE CT domain to (i) define the binding location of Aβ on apoE CT by fluorescence resonance energy transfer (FRET) analysis and (ii) determine the effect of Aβ interaction on the ability of apoE to bind lipid surfaces. We demonstrate that Aβ interacts with the hydrophobic lipid binding sites of apoE CT and that the interaction with Aβ compromises the lipid binding ability of apoE CT.

EXPERIMENTAL PROCEDURES

Materials. *N*-Iodoacetyl-*N*′-(5-sulfo-1-naphthyl)ethylenediamine (AEDANS) and phospholipase C (PLC) from *Bacillus cereus* were obtained from Sigma-Aldrich (St. Louis, MO). A$\beta_{1–42}$ and fluorescein-A$\beta_{1–42}$ were from American Peptide Company (Sunnyvale, CA) and will be referred to as Aβ and fluorescein-Aβ, respectively. Anti-human apoE monoclonal antibody (3H1) was obtained from the Ottawa Heart Institute Research Corporation (Ottawa, Canada). Anti-Aβ antibody, 6E10, was obtained from Signet Laboratories, Inc. (Dedham, MA). The rabbit (polyclonal) anti-oligomer antibody (A11) was from BioSource (Camarillo, CA) (*23*). Dimyristoylphosphatidylcholine (DMPC) was obtained from Avanti Polar Lipids (Alabaster, AL). Human LDL was obtained from Intracel Resources (Frederick, MD). The phospholipid assay kit was from Wako Chemicals USA, Inc. (Richmond, VA).

Expression and Purification of ApoE CT Variants. Wild-type (WT) human recombinant apoE CT encompassing residues 201–299 was expressed in *Escherichia coli* as described earlier (*24*) with a His tag at the N-terminal end to facilitate purification. ApoE CT containing a single Cys residue at position 209, 223, 255, or 277 was generated using the QuikChange site-directed mutagenesis kit (Stratagene, La Jolla, CA). The proteins were purified under denaturing conditions from cell lysates using a His-Trap HP column (GE Health Care, NJ). Quantitative protein analysis was carried out by the DC protein assay (Bio-Rad Laboratories, Hercules, CA).

AEDANS Labeling of ApoE CT Variants. Single Cys containing apoE CT variants were labeled with AEDANS as described previously (*25*). The stoichiometry of labeling was 1:1 apoE CT/AEDANS as calculated from the molar extinction coefficient of AEDANS (5.7×10^3 cm^{-1} M^{-1}).

Preparation of Phospholipid/ApoE CT Lipoprotein Complexes. Reconstituted lipoproteins containing phospholipids and apoE CT (also called lipid-bound complexes of apoE CT) were prepared by incubating 2.5 mg of DMPC multilamellar vesicles (MLVs) with 1 mg of apoE CT (50:1, initial lipid/apoE CT molar ratio) at 24 °C for 16 h. The samples were subjected to density-gradient ultracentrifugation (65000*g*) for 4 h and fractionated to separate lipid-bound from unbound apoE CT. The resultant lipid-bound complexes of apoE CT are well-characterized particles that have been used in previous studies (*24, 26*). They are ~17 nm in diameter, discoidal in geometry, bear a final lipid/apoE CT molar ratio of ~130:1 with 4–6 apoE CT/particle, and broadly resemble nascent discoidal high-density lipoprotein (HDL) in size and shape. The lipid content of the particles was determined using the phospholipid assay kit.

Oligomeric Aβ Preparation. Oligomeric Aβ was prepared essentially as described by established protocols (*23, 27*). After initial solubilization in hexafluoroisopropanol, Aβ was diluted to a 50–100 μM concentration in 50 mM Tris-HCl and 100 mM NaCl at pH 7.4 (buffer A) and incubated at 4 or 24 °C for 24 h. This treatment yielded oligomeric Aβ preparations as deduced by positive reactivity with the oligomer-sensitive antibody A11 by dot blot analysis (*23*). This procedure was adopted systematically to ensure that each Aβ preparation will start with the same initial state and that they do not retain any "structural history". When fluorescein-Aβ was involved, it was a mixture of a 1:3 weight ratio of fluorescein-Aβ with unlabeled Aβ and will be simply referred to as fluorescein-Aβ. In previous studies, the oligomerization behavior of fluorescein-A$\beta_{1–40}$ was reported to be similar to that of WT A$\beta_{1–40}$ (*28*).

FRET Analysis. Lipid-free or lipid-bound AEDANS-labeled apoE CT variants were incubated in the absence or presence of fluorescein-Aβ in buffer A at 4 °C for 24 h (20:1 weight ratio of apoE CT/Aβ). The AEDANS moiety served as the FRET donor, while fluorescein (located at the N-terminal end at position 1 of Aβ) was the acceptor. The excitation and emission wavelengths for AEDANS-labeled apoE CT variants were 345 and ~485 nm, respectively. The excitation and emission wavelengths for fluorescein-Aβ were 485 and 520 nm, respectively. Fluorescence emission spectra of the mixtures were recorded between 400 and 600 nm (excitation at 345 nm), with the excitation and emission slit widths set at 5 nm. Fluorescence emission of oligomeric fluorescein-Aβ alone in the absence of AEDANS-labeled apoE CT was subtracted following direct excitation at 345 (optimal excitation wavelength for AEDANS) for FRET analysis to follow sensitized emission because of FRET alone from AEDANS on apoE CT to fluorescein-Aβ. Fluorescence analyses were carried out on a LS50B Perkin-Elmer luminescence spectrometer.

Lipid Binding Assay. A characteristic functional feature of apolipoproteins is their ability to transform phospholipid vesicles into discoidal bilayer complexes resembling nascent HDL. This ability has been employed routinely to evaluate the lipid binding ability of apolipoproteins (*29, 30*) from observations involving the initial kinetics of transformation. Briefly, DMPC MLVs were prepared in 20 mM Tris-HCl at pH 7.4 and 150 mM NaCl (Tris-buffered saline, TBS). DMPC vesicles (100 μg as determined by the phospholipid assay kit) were equilibrated at 24 °C, followed by the addition of 10 μg of apoE CT or 10 μg of apoE CT preincubated with 10 or 100 μg of oligomeric Aβ at 4 °C for 24 h or 100 μg of oligomeric Aβ alone. To examine if the presence of Aβ affected the lipid binding behavior of apolipoproteins other than apoE, we compared the behavior of recombinant human apoAI bearing a His tag (purified as described for apoE CT) under similar conditions. The decrease in turbidity accompanying the transformation of MLVs to the smaller discoidal complexes was followed as a decrease in the absorbance at 325 nm for 60 min. The measurements were performed in a Perkin-Elmer spectrophotometer maintained at 24 °C in a Peltier-controlled (PTP-6) cell holder. The $T_{1/2}$ (time required for a 50% decrease in the initial absorbance) and the rate constant, K (calculated as reciprocal of $T_{1/2}$), were calculated for the vesicles to discs transformation process.

Binding to Spherical Lipoproteins. The effect of Aβ interaction on the binding of apoE CT to spherical lipoprotein particles was measured as previously described (*31*). In the present study, 50 μg of human LDL was treated with PLC (75 mU) in the absence or presence of 5 μg of apoE CT in 50 mM Tris-HCl at pH 7.4, 150 mM NaCl, and 2 mM $CaCl_2$. Further, apoE CT was preincubated with 0 or 20 μg of oligomeric Aβ at 4 °C for 24 h, prior to addition to the LDL. The reaction was initiated by the addition of PLC followed by incubation at 37 °C in a microtiter plate. The aggregation was monitored at regular intervals as changes in the solution turbidity at 340 nm.

Immunoblot. Western blot analyses were performed using anti-apoE or anti-Aβ antibodies 3H1 or 6E10, respectively. Dot blot analysis was performed to confirm the oligomeric nature of unlabeled and fluorescein-Aβ using the oligomer-specific antibody A11 (1:1000 dilution). The secondary antibodies used were anti-mouse and anti-rabbit IgG horseradish peroxidase-conjugated antibody (Chemicon) (1:10 000 dilution). ECL Western blot detection kit (GE Healthcare) was used to detect the chemiluminescence.

RESULTS

Rationale and Design of ApoE CT Variants. Previous studies indicate that the C-terminal end of apoE encompasses tandem segments (216–266 and 273–299) that have a propensity to form an α-helical conformation (*6*). Further, our studies suggest that residues 218−266 are likely involved in a coiled-coil interhelical dimer formation (*24*). The dimerization model aids in sequestering the hydrophobic lipoprotein binding sites in the lipid-free state (underlined, solid line in Figure 1), while residues 273–299 aid in apoE self-association (*32*) (underlined, dashed line in Figure 1), causing dimerization of the dimer. The lipoprotein binding and self-association sites probably overlap. Additionally,

QPLQERAQ**A**W GERLRARMEE MG**S**RTRDRLD
EVKEQVAEVR AKLEEQAQQI RLQA**E**AFQAR
LKSWFEPLVE DMQRQW**A**GLV EKVQAAVGTS
AAPVPSDNH

FIGURE 1: Primary structure of apoE CT. ApoE (201–299) encompasses the entire apoE CT domain. The putative lipoprotein binding sites are underlined with a solid line, and the self-association sites are underlined with a dashed line. The lipoprotein binding and self-association sites probably overlap. The sites probed (at positions 209, 223, 255, and 277) for Aβ binding location are shown in bold.

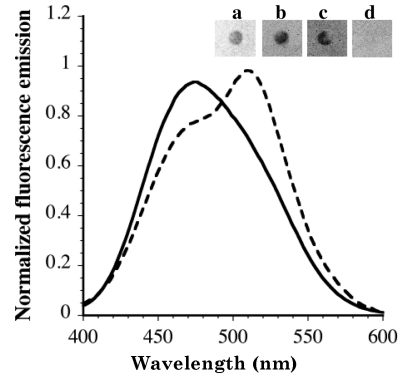

FIGURE 2: FRET between lipid-free AEDANS-S223C/apoE CT and fluorescein-Aβ. Fluorescence emission spectra of AEDANS-S223C/apoE CT in the absence (—) or presence (- - -) of fluorescein-Aβ were recorded between 400 and 600 nm following excitation at 345 nm in TBS. The excitation and emission slit widths were set at 5 nm. (Inset) Dot blot analysis of fluorescein-Aβ. The fluorescein moiety is located at the N-terminal end at position 1 of $A\beta_{1-42}$. The antioligomer antibody, A11, was used as described under the Experimental Procedures. The designations are as follows: as described under the Results, fluorescein-Aβ (a) or unlabeled Aβ (b) was incubated in buffer A; unlabeled Aβ was incubated in F12 medium (c); and unlabeled Aβ was incubated at 24 °C for 7–21 days in 10 mM HCl (d).

other papers suggest that apoE CT is one of the potential sites of interaction for Aβ (*12, 33–36*). Four single cysteine variants of apoE CT were generated, with the cysteine located at position 209, 223, 255, or 277 (Figure 1). Because WT apoE CT lacks cysteine residues, the substituted cysteine provides a unique site for site-specific fluorescence labeling with AEDANS. The labeling efficiency was calculated to be ~95% for all four variants. Circular dichroism analysis revealed that the secondary-structure content, unfolding behavior, and the overall fold of the unlabeled and AEDANS-labeled variants were identical to those of the WT protein; additionally, the lipid binding affinity of the variants were similar to that of the WT protein (data not shown).

AEDANS-labeled single Cys variants of apoE CT were incubated in the absence or presence of fluorescein-Aβ (20:1 weight ratio of apoE CT/Aβ). We ensured that the fluorescein-Aβ was oligomeric under the conditions employed (incubation in buffer A at 24 °C for 24 h) using dot blot analysis with the antioligomer antibody (inset in Figure 2). As positive controls, we used unlabeled Aβ in buffer A or F12 medium at 24 °C for 24 h as described by others (*23, 27*). Finally, as a negative control, we incubated Aβ at 24 °C for 7–21 days in 10 mM HCl; this treatment yielded fibrillar species that are not detected by the oligomer-specific antibody.

When the oligomeric nature of the fluorescein-Aβ was confirmed, the fluorescence emission spectra of mixtures containing AEDANS-apoE CT variants and oligomeric

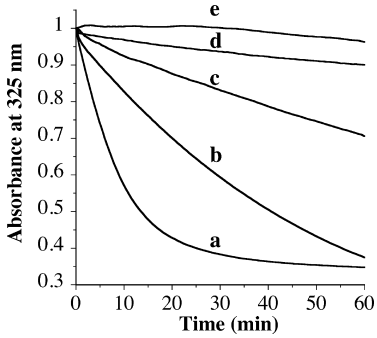

FIGURE 3: Effect of Aβ on the ability of apoE CT to transform phospholipid vesicles to discoidal complexes. DMPC MLVs (100 μg) were treated with 10 μg of apoE CT (curve a), 10 μg of apoE CT that was preincubated with 10 μg (curve b) or 100 μg (curve c) of oligomeric Aβ, or 100 μg of oligomeric Aβ alone (curve d) in TBS. The change in absorbance at 325 nm was followed at 24 °C as a function of time and is shown as normalized absorbance units. In the absence of protein, there was no change in the absorbance of the vesicles alone (curve e). Representative curves from four different experiments are shown.

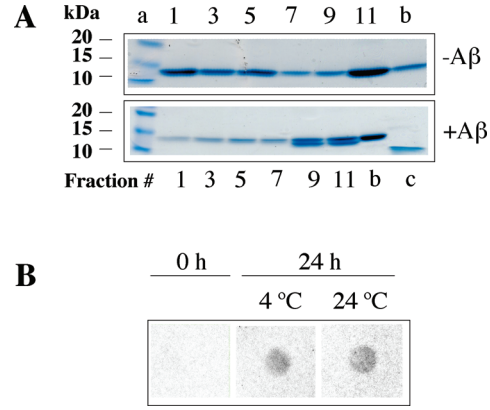

FIGURE 4: Effect of Aβ in apoE CT/lipid mixtures on the extent of lipid-associated apoE CT. (A) SDS−PAGE analysis: 4–20% acrylamide gradient SDS−PAGE analysis of density-gradient ultracentrifugation fractions (fractions 1, 3, 5, 7, 9, and 11) was carried out on incubations containing lipid-free apoE CT (1 mg) and phospholipid vesicles (2.5 mg of lipid) in the absence (top) or presence (bottom) of 50 μg of Aβ at 24 °C for 24 h. Lane a, molecular mass standards; lane b, lipid-free apoE CT; and lane c, free Aβ. (B) Dot blot analysis: 10 μg of Aβ was incubated at 4 or 24 °C for 24 h in buffer A, followed by dot blot analysis with the antibody A11. The status of Aβ prior to the incubation period is shown for comparison.

fluorescein-Aβ were recorded following incubation. Figure 2 shows representative fluorescence emission spectra of AEDANS-S223C/apoE CT in the absence and presence of fluorescein-Aβ. Upon excitation at 345 nm, the fluorescence emission spectrum of AEDANS-S223C/apoE CT displays a maximal fluorescence emission at 460 nm. In the presence of fluorescein-Aβ, a decrease in the AEDANS fluorescence emission was noted, accompanied by the appearance of fluorescein fluorescence emission at ~520 nm, attributed to intermolecular FRET. The efficiency of energy transfer between AEDANS placed at defined sites on apoE CT and fluorescein located at the N-terminal end of Aβ was calculated as $E = 1 - I_{DA}/I_D$, where I_{DA} and I_D are the fluorescence emission intensities of the donor in the presence and absence of an acceptor, respectively. The efficiency of energy transfer was calculated to be 6%. Similar analysis with apoE CT bearing AEDANS located at positions 209 and 255 revealed energy-transfer efficiencies of 6.5 and 6%, respectively. However, the efficiency was found to be lower (1–3%) in the case of AEDANS located at position 277.

Because the binding location of Aβ appears to coincide with the lipoprotein binding and self-association surfaces of apoE (Figure 1), we investigated the functional consequence of this interaction on the lipid binding capability of apoE CT. Two different lipid binding assays were employed: assessment of the ability to transform phospholipid bilayer vesicles into discoidal complexes and evaluation of the ability to interact with spherical lipoprotein particles. The transformation of vesicles to discoidal complexes is manifest as a time-dependent decrease in turbidity, which is monitored at 325 nm. ApoE CT caused rapid transformation of the vesicles to discoidal lipoprotein complexes, with the end point approaching around 60 min (curve a in Figure 3). The $T_{1/2}$ (time required for a 50% decrease in the initial absorbance) and the rate constant, K (reciprocal of $T_{1/2}$), were calculated to be 14 and 0.07 min^{-1}, respectively. However, when apoE CT was preincubated with 10 or 100 μg of oligomeric Aβ (curves b and c in Figure 3, respectively), a decrease in the efficiency of transformation was noted. This was reflected as increases in $T_{1/2}$ to 41 and >60 min, respectively. In control incubations with Aβ (i.e., in the absence of apoE CT), there was no decrease in the absorbance of the vesicles, indicating that Aβ does not have the ability to convert vesicular bilayer structures to discoidal bilayer complexes, even at 100 μg, the highest concentration used in this study (curve d in Figure 3). In the absence of added apolipoproteins, the absorbance of the vesicles at 325 nm remains unchanged (curve e in Figure 3). To examine if Aβ affected the lipid binding behavior of apolipoproteins other than apoE, we employed apoAI, an exchangeable apolipoprotein with high lipid binding affinity (*37*). We observed that far less apoAI (4 μg) was required to transform MLVs at rates comparable to that of apoE CT and that Aβ did not alter the ability of apoAI to cause transformation (data not shown).

We then assessed the end product of the reaction between apoE CT and lipid vesicles to assess if the decreased initial binding rates resulted in lesser amounts of lipid-associated apoE CT. The assay described for Figure 3 was performed on a larger scale, and apoE CT was incubated with phospholipid vesicles in the absence or presence of Aβ at 24 °C for 24 h, followed by density-gradient ultracentrifugation and fractionation. Sodium dodecyl sulfate−polyacrylamide gel electrophoresis (SDS−PAGE) of the fractions (Figure 4A) reveals the presence of apoE CT in the (top) lipoprotein-containing fractions in the absence of Aβ. However, in the presence of oligomeric Aβ, a significantly lower amount of apoE CT was noted in the top fractions, while the bottom fraction had more apoE CT, reflecting the presence of lipid-free protein. The additional band of higher mobility noted in fractions 9 and 11 is attributed to the presence of oligomeric (dimeric/trimeric) Aβ that is not associated with lipid. The presence of oligomeric Aβ under these conditions was confirmed by dot blot analysis using the antioligomer antibody (Figure 4B). This result was confirmed in a parallel experiment using fluorescein-Aβ to monitor the presence of Aβ (data not shown).

To independently confirm that Aβ interaction affects the lipid binding behavior of apoE CT, we monitored the binding

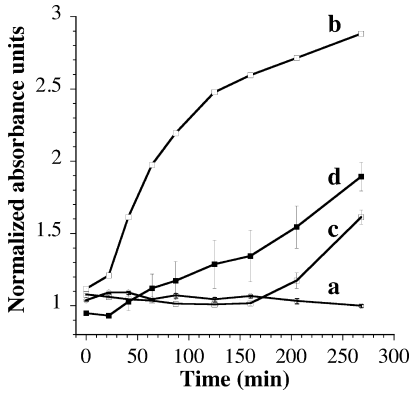

FIGURE 5: Effect of Aβ on the ability of apoE CT to protect PLC-treated LDL against aggregation. Human LDL (50 μg) was incubated at 37 °C for varying lengths of time as such (curve a) or with 75 mU PLC (curve b) and the following additions in 50 mM Tris-HCl at pH 7.4, 150 mM NaCl, and 2 mM $CaCl_2$: 5 μg of apoE CT (curve c) and 5 μg of apoE CT plus 20 μg of oligomeric Aβ (curve d). The absorbance was measured at 340 nm at various time intervals. Values have been normalized to the absorbance at the 0 min time point and expressed as an average ± standard deviation (SD) ($n = 3$).

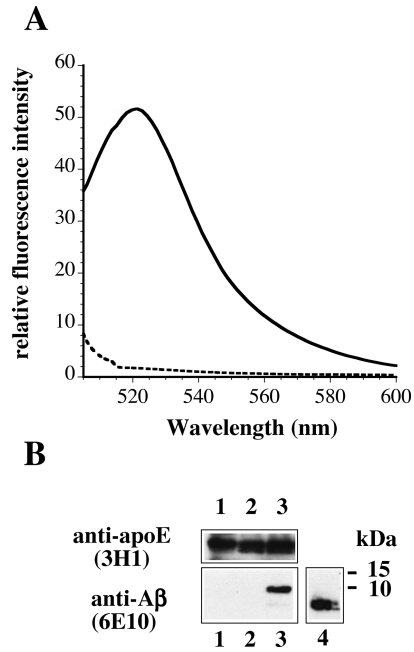

FIGURE 6: Partitioning of Aβ into lipoprotein particles bearing WT apoE CT. (A) Fluorescence emission spectra of apoE CT-containing lipoproteins in the absence or presence of fluorescein-Aβ. WT apoE CT-containing lipoprotein particles were incubated with buffer or oligomeric fluorescein-Aβ (20:1 weight ratio of apoE CT/Aβ) at 4 °C for 24 h. The lipoprotein particles were reisolated by density-gradient ultracentrifugation to separate unbound from lipoprotein-bound Aβ. Fluorescence emission spectra of lipoprotein particles were recorded in the absence (• • •) and presence (—) of fluorescein-Aβ (excitation at 495 nm, excitation and emission slit widths were set at 5 nm). (B) Western blot analysis of apoE CT-containing lipoproteins in the absence or presence of Aβ. Western blot analysis of pooled lipoprotein fractions was performed in the absence (lane 2) and presence (lane 3) of Aβ, using anti-apoE antibody 3H1 (top) or anti-Aβ antibody 6E10 (bottom). Lipid-free apoE CT and monomeric Aβ are shown as controls in lanes 1 and 4, respectively.

by an assay described earlier using spherical lipoprotein particles (*31, 38*). The assay is based on the ability of apolipoproteins to prevent PLC-induced aggregation of LDL particles. In the absence of additives, LDL is stable in buffer over the time period of the assay (curve a in Figure 5). PLC causes a time-dependent increase in LDL turbidity, which is expressed as the lag period. The lag period (expressed in minutes) is obtained by extrapolating the slope of the curve to intersect the *x* axis. The increase in turbidity is attributed to LDL aggregation because of the exposure of diacylglycerol moieties generated as a result of PLC-induced cleavage of the phosphocholine head groups in the monolayer of the LDL. In the presence of PLC, LDL aggregation occurred with a lag period of ~10 min (curve b in Figure 5). In the presence of apoE CT, a significant delay in the onset of aggregation occurred (160 min) (curve c in Figure 5), which is interpreted as a result of the binding of apoE CT to the exposed hydrophobic surface on the LDL created by PLC. However, if apoE CT was pretreated with oligomeric Aβ, the lag period decreased to about 40 min (curve d in Figure 5) and the ability of apoE CT to afford protection against aggregation was significantly reduced. The decreased lag period suggests that the interaction with Aβ significantly impairs the ability of apoE CT to bind lipid surfaces. Together, the results suggest the following: (i) Aβ associates with apoE at the hydrophobic lipoprotein binding site(s) in the CT domain, and (ii) Aβ association with apoE CT decreases the overall lipid binding ability of apoE CT and results in lowered levels of lipid-associated apoE CT.

The next step was to examine if Aβ partitions into a lipoprotein particle. Lipid-bound complexes of WT apoE CT were treated with buffer or fluorescein-Aβ (20:1 weight ratio of apoE CT/Aβ) at 4 °C for 24 h. The lipoprotein complexes were reisolated by density-gradient ultracentrifugation to separate lipoprotein bound from unbound Aβ. Fluorescence analysis (direct excitation at 495 nm) of the top fraction revealed the fluorescence emission characteristics of fluorescein (Figure 6A) (wavelength of maximal emission intensity at ~520 nm), indicative of the association of Aβ with the lipoprotein particles. The partitioning was independently confirmed by Western blot analysis of the lipoprotein fractions using anti-apoE antibody 3H1 (top of Figure 6B) and anti-Aβ antibody 6E10 (bottom of Figure 6B). It should be noted that the mobility of Aβ in the lipoprotein fractions (lane 3) corresponds to that of a SDS-stable oligomer (dimer or trimer) (free monomeric Aβ shown in lane 4 for comparison). The resultant lipoprotein particles are ~17 nm in diameter, with a lipid/apoE/Aβ molar ratio of 350:3:1.

Having established that Aβ partitions into the lipoprotein particle, it was essential to see if it interacts with the protein component or if it is localized in the lipid environment of the particle. Previous studies indicated that full-length apoE (*25*) and its isolated NT (*39, 40*) and CT (*24*) undergo a conformational change when the lipid-free protein interacts with lipids. In the lipid-bound state, apoE adopts an extended helical conformation, with the α helices circumscribing the phospholipid bilayer, and the helical axes parallel to the plane of the bilayer (*26, 39, 41, 42*). The nonpolar faces of the amphipathic helices are apposed to the hydrophobic fatty acyl chains of the phospholipid bilayer. It can therefore be envisaged that apoE CT presents an equitable nonpolar continuum for potential interaction for the lipid-associated Aβ at the protein/lipid interface of the particle.

To investigate the possibility of direct interaction between Aβ and the protein component of the lipoprotein, intermo-

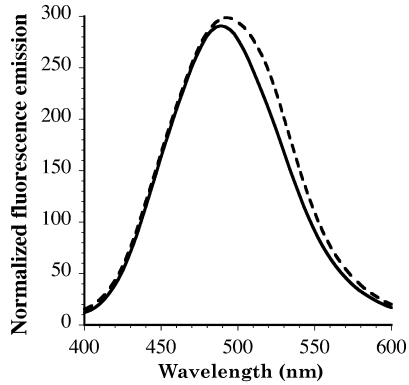

FIGURE 7: FRET between lipid-bound AEDANS-A277C/apoE CT and fluorescein-Aβ. Fluorescence emission spectra of lipid-bound AEDANS-A277C/apoE CT were recorded in the absence (—) or presence (- - -) of fluorescein-Aβ between 400 and 600 nm following excitation at 345 nm in TBS. The excitation and emission slit widths were set at 5 nm.

Table 1: Effect of Lipid Binding and Fluorescein-Aβ Addition on the Wavelength of Maximal Fluorescence Emission Intensity of AEDANS-Labeled ApoE CT Variants

	wavelength of maximal fluorescence emission intensity (λ_{max}) (nm)			
	lipid free		lipid bound	
	−Aβ	+Aβ	−Aβ	+Aβ
A209C	467	468	482	482
S223C	470	470	485	485
E255C	469	469	487	487
A277C	479	480	486	486

lecular FRET analysis was carried out between fluorescein-Aβ and lipid-associated apoE CT variants bearing AEDANS at positions 209, 223, 255, or 277. Fluorescence emission spectra of the mixtures were recorded following excitation at 345 nm. FRET was uniformly absent or negligible in all of the variants studied regardless of the location of the probe, suggesting the lack of direct binding interaction between lipid-associated apoE CT and Aβ. An example with lipid-associated AEDANS-A277C/apoE CT and fluorescein-Aβ is shown in Figure 7. It appears that Aβ loses specificity to a particular binding region on lipid-associated apoE CT. Because Aβ was found to partition into the lipoprotein particles, we conclude that it is present in the lipid milieu of the lipoprotein. Further, no changes in the wavelength of maximal fluorescence emission intensity (λ_{max}) were noted for AEDANS in the different variants because of fluorescein-Aβ addition (Table 1). It appears that the microenvironment of the AEDANS probe at each location is not grossly altered upon Aβ interaction.

DISCUSSION

Our recent studies indicate that the CT domain of apoE promotes ATP-binding cassette transporter A1-mediated cholesterol efflux as efficiently as apoAI and is essential and necessary for HDL particle assembly (*43*). We proposed that the hydrophobic helical segments of this domain determined the efficiency of cholesterol efflux. The CT domain is composed of amphipathic α-helical segments that present a large hydrophobic surface (*4, 44*) for potential interaction with lipids. It bears high-affinity lipid binding sites that can initiate lipoprotein binding interaction. This initial interaction between apoE and lipoproteins plays a significant role in anchoring apoE to the lipoprotein, a feature that is considered an *a priori* requirement for apoE to serve as a ligand for the LDL receptor and the subsequent clearance of the particles (*45, 46*). The apoE CT domain encompasses two types of amphipathic helices (*6*): class A (residues 216–266), which makes intermolecular helix−helix contacts that aids in sequestration of hydrophobic sites mediating dimerization (*24*), and class G* helix (residues 273–299), which promotes apoE self-association. Previous papers suggest that Aβ interacts with the CT domain of apoE (*13, 33–36, 47*). The objectives of the present study are to identify the location of binding of the oligomeric Aβ on apoE CT and to test the hypothesis that interaction with Aβ impairs the lipid binding function of apoE CT.

The levels of soluble oligomeric Aβ and not of the fibrillar Aβ are correlated directly with cognitive decline, neuronal toxicity, and the severity of the disease (*9, 10, 48*). Their levels are significantly increased in the brains of AD patients (*49*). Oligomeric Aβ appears to be the predominantly stable species under physiological conditions (*28, 50*) and are sufficient and necessary to impair cognitive function and learning behavior (*51*).

Previously, we took advantage of the intrinsic fluorescence properties of apoE CT because of the naturally occurring Trp residues (at positions 210, 264, and 276) to evaluate its interaction with Aβ (*36*). However, because of the fluorescence contribution of the three Trp residues, we were unable to discern the binding location of Aβ to specific helical segments within the CT domain. In the present study, we probed specific helical segments: positions 223 and 255 to probe the two ends of the class A helix (216–266) and position 277 to monitor the class G* helix (273–299); in addition, we placed a probe at position 209 to monitor the segment preceding the class A helix. The presence of the probe did not affect the structural or functional behavior of the protein. The likelihood that its presence affects Aβ interaction with apoE is also small because we believe that Aβ interacts at more than a single site on apoE CT (discussed below). While FRET was noted with the probes at each of the selected locations, the efficiency of FRET with the probes at positions 209, 223, and 255 was twice as high as that with the variant bearing a probe at position 277 in lipid-free apoE. Thus, it appears that Aβ binding spans the entire segment between residues 209 and 255. This putative Aβ binding location overlaps with the lipoprotein binding sites (*32*) and helix−helix contact sites (*24*) reported for apoE. Employing C-terminal truncation variants of apoE, it was indicated that the lipoprotein binding sites reside in the vicinity of residues 220–266 (*32*). Figure 8 represents apoE CT residues 216–291 as a helical net, showing the arrangement of the hydrophobic and polar residues. The hydrophobic continuum of amino acids involved in lipoprotein and self-association interactions likely present an optimal surface for the interaction with oligomeric Aβ in lipid-free apoE. We can then anticipate two outcomes in this situation: (i) that the lipid or lipoprotein binding ability of apoE CT pretreated with Aβ will be impaired, and (ii) if apoE CT is already bound to lipids, that Aβ can either interact with the lipid or the protein component of the lipoprotein particle. Because the sequence of apoE is identical in the CT domain of apE3 and apoE4 isoforms, the data obtained with the isolated CT

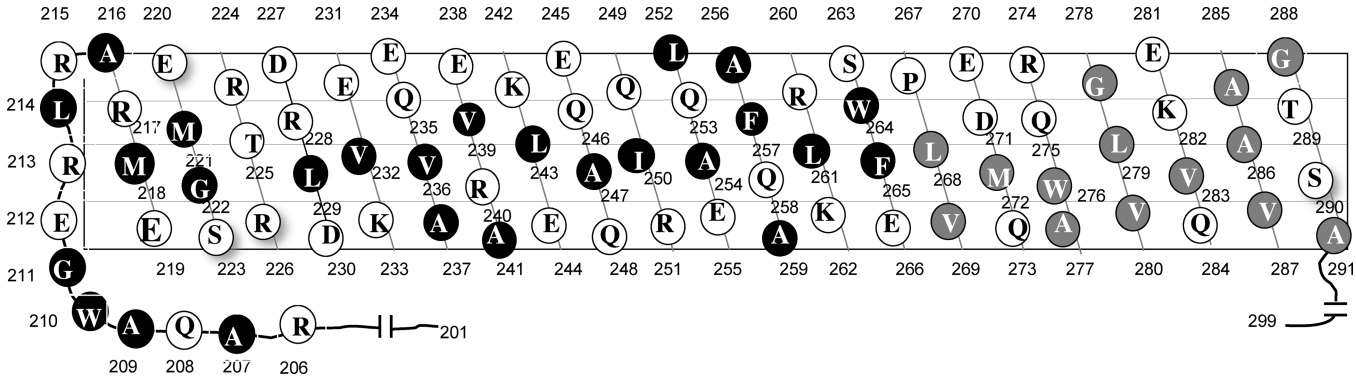

FIGURE 8: Putative Aβ binding location in the apoE CT. Secondary-structure algorithms suggest that the CT of apoE is likely folded into a series of amphipathic α helices. Residues 216–291 are represented as a continuous α-helical net (~3.6 residues/turn). The polar residues are shown as white circles. The hydrophobic residues are shaded black in the class A helix (housing the major lipoprotein binding sites and apoE dimerization sites) and gray in the class G* helix (housing the major apoE self-association sites). The putative binding location for Aβ is believed to coincide with the shaded hydrophobic residues.

domain may be extended to the intact proteins. However, a caveat to this observation is that a domain interaction in lipid-free apoE4 but not in apoE3 (*52*) is believed to determine various biochemical, biophysical, and possibly physiological behavior of apoE4 (*44*). The domain interaction is comprised of a salt bridge between Arg61 in the NT domain and Glu255 in the CT domain of apoE4. Further, the spatial proximity between these two residues appears to be retained in the lipid-bound state (*42, 53*). More studies are needed to evaluate the possibility that the lipid-associated conformation of the isolated apoE CT domain resembles that of the corresponding segment in lipid-associated intact apoE3 and/or apoE4.

As anticipated from the biophysical analysis, the presence of Aβ decreases the ability of lipid-free apoE CT to bind lipids. Although apoE is believed to be predominantly lipid-bound in a physiological situation, the possible contribution of the lipid-free protein cannot be ignored. Studies carried out with human monocyte-macrophages demonstrate that apoE (i) is constitutively secreted, (ii) does not leave the macrophages with lipid, and (iii) forms discoidal particles with buoyant density, 1.08–1.1 g/mL, following enrichment of macrophages with cholesterol (*54*). The lipidated status of secreted apoE appears to vary with the cell type used: in some types, only ~10 or 20% of secreted apoE are lipid-associated (*55, 56*), while in others, it is mostly lipid-associated following cholesterol enrichment of the cells (*57–59*). Finally, the observation that apoE fragments have been identified in the brain (see discussion below) suggests that lipid-free apoE may be present *in vivo*. In the present study, the interaction of apoE CT with two types of lipid surfaces was followed: phospholipid bilayer vesicles and phospholipid monolayer of spherical lipoprotein particles. In the vesicles to discoidal lipoprotein transformation assay, the presence of Aβ dramatically decreased the initial binding rates of apoE CT. The interaction with Aβ also decreases the overall amount of lipid-associated apoE CT following extended incubations. In addition, Aβ significantly decreases the ability of apoE CT to interact with the hydrophobic surface created in the phospholipid monolayer of the spherical particle. The end products of the two assays recapitulate the overall geometry of apoE-containing discoidal and spherical HDL-sized particles that have been described for lipoproteins associated with the CNS (*60*). There are no reports of triglycerides containing lipoproteins in the brain, and only HDL-sized lipoproteins are believed to serve the cholesterol delivery function in this organ. Lipid binding of apolipoproteins is an essential step in the generation of lipoproteins; this step also marks a lipoprotein for cellular clearance via receptor-mediated endocytosis. Thus, the physiological implication for our observations is that interaction with Aβ likely decreases the extent of the assembly and formation of apoE-containing HDL. ApoE is the major apolipoprotein identified in the brain that plays a predominant role in cholesterol delivery to the neurons (*5*), which is required for synaptogenesis. Thus, the consequences of impaired HDL assembly are poor cholesterol delivery and synapse formation.

Lipid-bound apoE CT presents a different scenario for Aβ interaction: Aβ partitions into the lipoprotein particle yielding complexes that are ~690,000 Da in molecular mass and ~17 nm in particle diameter, with a lipid/apoE/Aβ molar ratio of ~350:3:1. In these discoidal complexes, apoE CT is expected to circumscribe the periphery of the lipoprotein particle in an extended helical conformation, with the helical axes oriented perpendicular to the plane of the bilayer (*26*). However, because FRET was uniformly low regardless of the location of the probe on apoE CT, we conclude that Aβ is located in the lipid milieu and does not interact directly with the protein component of the lipoprotein. An alternative explanation is that the AEDANS moiety faces away from the lipid milieu in the lipid-bound apoE CT variants. Indeed, upon lipid association, the fluorescence emission of AEDANS-labeled apoE CT variants displayed a shift toward higher wavelengths (Table 1). This red shift suggests that the AEDANS moiety was localized in a relatively hydrophobic microenvironment in lipid-free apoE CT, and they likely face the aqueous environment in the lipid-bound protein. However, there were no changes in the λ_{max} upon the addition of Aβ in either the lipid-free or -bound states. We conclude that there were no Aβ-induced local changes in the microenvironment of AEDANS at the different locations. The implication of this observation is that sequestration of Aβ in the apoE CT-containing lipoprotein particle can potentially lead to increased extracellular accumulation. This is because the isolated apoE CT domain (which does not bear the LDL receptor binding sites) cannot mediate cellular particle clearance via cell-surface-localized lipoprotein receptors.

Interestingly, apoE and its fragments have been identified in the amyloid plaques in the AD brain (*61, 62*). The 22

kDa amino-terminal fragment of apoE has been shown to bear intense neurotoxic properties (*63, 64*). In addition, fragments encompassing residues 187–299 were identified in neuroblastoma cells overexpressing apoE (*65*), while apoE fragments corresponding to residues 216–299 and 193–299 were identified in the amyloid plaques of postmortem AD brains. It is not known if the apoE fragments were generated prior to or after interaction with Aβ. Further, considering that lipid-free apoE is more susceptible to protease activity than lipid-bound apoE (the protease-sensitive loop linking the two domains is shielded in the lipid-bound state) (*3, 41*), the presence of apoE fragments suggests that the fragments could have originated from lipid-free apoE. It has been indicated that apoE4 is relatively more susceptible to protease digestion compared to apoE3. It is thus likely that the neurotoxicity associated with apoE4 may be due to the generation of the apoE4 NT and the CT fragments: the NT fragment being neurotoxic (*63*) and the CT domain interacting with Aβ that cannot be cleared from extracellular sites. Indeed, the CT fragment has been suggested to play a role in inducing and stabilizing the formation of the oligomeric form of Aβ (*65*). These earlier studies provide direct physiological relevance for our biophysical analysis.

Although the CT sequence is identical in apoE2, apoE3, and apoE4, the interaction between the N- and C-terminal domains that has been suggested for apoE4 (*52*) will play a predominant role in determining Aβ binding with the intact protein. In the absence of Aβ, all three isoforms display similar lipid binding activity and stimulate cholesterol efflux to a comparable extent (*43*). Despite several efforts to determine the binding location of Aβ on apoE, there appears to be little consensus: some report a binding preference for the C-terminal domain (*13, 33, 47*), while others note a preference for the N-terminal domain (*66*), and yet others suggest binding in both domains (*34, 35, 67*). The large conformational differences between lipid-free and lipid-associated states of apoE and possibilities of numerous conformations between these states depending upon the type and extent of lipidation likely explain the differences in observations from different groups regarding Aβ binding. Further studies in defining the Aβ binding location precisely in the intact protein and in determining its effect on the overall function of apoE will be crucial in understanding the role of apoE in amyloid pathology.

ACKNOWLEDGMENT

We thank Dr. Victor Drover, Medical College of Wisconsin, Milwaukee, WI, for generating the graphic for the Table of Contents.

REFERENCES

1. Raffai, R. L., and Weisgraber, K. H. (2003) Cholesterol: From heart attacks to Alzheimer's disease. *J. Lipid Res. 44*, 1423–1430.
2. Wetterau, J. R., Aggerbeck, L. P., Rall, S. C., Jr., and Weisgraber, K. H. (1988) Human apolipoprotein E3 in aqueous solution. I. Evidence for two structural domains. *J. Biol. Chem. 263*, 6240–6248.
3. Weisgraber, K. H. (1994) Apolipoprotein E: Structure−function relationships. *Adv. Protein Chem. 45*, 249–302.
4. Saito, H., Lund-Katz, S., and Phillips, M. C. (2004) Contributions of domain structure and lipid interaction to the functionality of exchangeable human apolipoproteins. *Prog. Lipid Res. 43*, 350–380.
5. Mauch, D. H., Nagler, K., Schumacher, S., Goritz, C., Muller, E. C., Otto, A., and Pfrieger, F. W. (2001) CNS synaptogenesis promoted by glia-derived cholesterol. *Science 294*, 1354–1357.
6. Segrest, J. P., Jones, M. K., De Loof, H., Brouillette, C. G., Venkatachalapathi, Y. V., and Anantharamaiah, G. M. (1992) The amphipathic helix in the exchangeable apolipoproteins: A review of secondary structure and function. *J. Lipid Res. 33*, 141–166.
7. Rensink, A. A., de Waal, R. M., Kremer, B., and Verbeek, M. M. (2003) Pathogenesis of cerebral amyloid angiopathy. *Brain Res. 43*, 207–223.
8. Selkoe, D. J. (1998) The cell biology of β-amyloid precursor protein and presenilin in Alzheimer's disease. *Trends Cell Biol. 8*, 447–453.
9. Naslund, J., Haroutunian, V., Mohs, R., Davis, K. L., Davies, P., Greengard, P., and Buxbaum, J. D. (2000) Correlation between elevated levels of amyloid β-peptide in the brain and cognitive decline. *J. Am. Med. Assoc. 283*, 1571–1577.
10. Kirkitadze, M. D., Bitan, G., and Teplow, D. B. (2002) Paradigm shifts in Alzheimer's disease and other neurodegenerative disorders: The emerging role of oligomeric assemblies. *J. Neurosci. Res. 69*, 567–577.
11. Huang, Y., Weisgraber, K. H., Mucke, L., and Mahley, R. W. (2004) Apolipoprotein E: Diversity of cellular origins, structural and biophysical properties, and effects in Alzheimer's disease. *J. Mol. Neurosci. 23*, 189–204.
12. Strittmatter, W. J., Saunders, A. M., Schmechel, D., Pericak-Vance, M., Enghild, J., Salvesen, G. S., and Roses, A. D. (1993) Apolipoprotein E: High-avidity binding to β-amyloid and increased frequency of type 4 allele in late-onset familial Alzheimer disease. *Proc. Natl. Acad. Sci. U.S.A. 90*, 1977–1981.
13. Strittmatter, W. J., Weisgraber, K. H., Huang, D. Y., Dong, L. M., Salvesen, G. S., Pericak-Vance, M., Schmechel, D., Saunders, A. M., Goldgaber, D., and Roses, A. D. (1993) Binding of human apolipoprotein E to synthetic amyloid β peptide: Isoform-specific effects and implications for late-onset Alzheimer disease. *Proc. Natl. Acad. Sci. U.S.A. 90*, 8098–8102.
14. Sanan, D. A., Weisgraber, K. H., Russell, S. J., Mahley, R. W., Huang, D., Saunders, A., Schmechel, D., Wisniewski, T., Frangione, B., and Roses, A. D. (1994) Apolipoprotein E associates with β amyloid peptide of Alzheimer's disease to form novel monofibrils. Isoform apoE4 associates more efficiently than apoE3. *J. Clin. Invest. 94*, 860–869.
15. Chan, W., Fornwald, J., Brawner, M., and Wetzel, R. (1996) Native complex formation between apolipoprotein E isoforms and the Alzheimer's disease peptide Aβ. *Biochemistry 35*, 7123–7130.
16. Zhou, Z., Smith, J. D., Greengard, P., and Gandy, S. (1996) Alzheimer amyloid-β peptide forms denaturant-resistant complex with type ε3 but not type ε4 isoform of native apolipoprotein E. *Mol. Med. 2*, 175–180.
17. Aleshkov, S., Abraham, C. R., and Zannis, V. I. (1997) Interaction of nascent apoE2, apoE3, and apoE4 isoforms expressed in mammalian cells with amyloid peptide β (1–40). Relevance to Alzheimer's disease. *Biochemistry 36*, 10571–10580.
18. Tokuda, T., Calero, M., Matsubara, E., Vidal, R., Kumar, A., Permanne, B., Zlokovic, B., Smith, J. D., Ladu, M. J., Rostagno, A., Frangione, B., and Ghiso, J. (2000) Lipidation of apolipoprotein E influences its isoform-specific interaction with Alzheimer's amyloid β peptides. *Biochem. J. 348*, 359–365.
19. Rebeck, G. W., Harr, S. D., Strickland, D. K., and Hyman, B. T. (1995) Multiple, diverse senile plaque-associated proteins are ligands of an apolipoprotein E receptor, the α2-macroglobulin receptor/low-density-lipoprotein receptor-related protein. *Ann. Neurol. 37*, 211–217.
20. LaDu, M. J., Shah, J. A., Reardon, C. A., Getz, G. S., Bu, G., Hu, J., Guo, L., and van Eldik, L. J. (2000) Apolipoprotein E receptors mediate the effects of β-amyloid on astrocyte cultures. *J. Biol. Chem. 275*, 33974–33980.
21. Beffert, U., Aumont, N., Dea, D., Lussier-Cacan, S., Davignon, J., and Poirier, J. (1998) β-Amyloid peptides increase the binding and internalization of apolipoprotein E to hippocampal neurons. *J. Neurochem. 70*, 1458–1466.
22. Hone, E., Martins, I. J., Jeoung, M., Ji, T. H., Ganady, S. E., and Martins, R. N. (2005) Alzheimer's disease amyloid-β peptide modulates apolipoprotein E isoform specific receptor binding. *J. Alzheimer's Dis. 7*, 303–314.
23. Kayed, R., Head, E., Thompson, J. L., McIntire, T. M., Milton, S. C., Cotman, C. W., and Glabe, C. G. (2003) Common structure of soluble amyloid oligomers implies common mechanism of pathogenesis. *Science 300*, 486–489.

24. Choy, N., Raussens, V., and Narayanaswami, V. (2003) Inter-molecular coiled-coil formation in human apolipoprotein E C-terminal domain. *J. Mol. Biol. 334*, 527–539.
25. Narayanaswami, V., Szeto, S. S., and Ryan, R. O. (2001) Lipid association-induced N- and C-terminal domain reorganization in human apolipoprotein E3. *J. Biol. Chem. 276*, 37853–37860.
26. Raussens, V., Drury, J., Forte, T. M., Choy, N., Goormaghtigh, E., Ruysschaert, J. M., and Narayanaswami, V. (2005) Orientation and mode of lipid-binding interaction of human apolipoprotein E C-terminal domain. *Biochem. J. 387*, 747–754.
27. Dahlgren, K. N., Manelli, A. M., Stine, W. B., Jr., Baker, L. K., Krafft, G. A., and LaDu, M. J. (2002) Oligomeric and fibrillar species of amyloid-β peptides differentially affect neuronal viability. *J. Biol. Chem. 277*, 32046–32053.
28. Garzon-Rodriguez, W., Sepulveda-Becerra, M., Milton, S., and Glabe, C. G. (1997) Soluble amyloid Aβ-(1–40) exists as a stable dimer at low concentrations. *J. Biol. Chem. 272*, 21037–21044.
29. Weers, P. M., Abdullahi, W. E., Cabrera, J. M., and Hsu, T. C. (2005) Role of buried polar residues in helix bundle stability and lipid binding of apolipophorin III: Destabilization by threonine 31. *Biochemistry 44*, 8810–8816.
30. Tamamizu-Kato, S., Wong, J. Y., Jairam, V., Uchida, K., Raussens, V., Kato, H., Ruyssachaert, J.-M., and Narayanaswami, V. (2007) Modification by acrolein, a component of tobacco smoke and age-related oxidative stress, mediated functional impairment of human apolipoprotein E. *Biochemistry 46*, 8392–8400.
31. Liu, H., Scraba, D. G., and Ryan, R. O. (1993) Prevention of phospholipase-C induced aggregation of low density lipoprotein by amphipathic apolipoproteins. *FEBS Lett. 316*, 27–33.
32. Westerlund, J. A., and Weisgraber, K. H. (1993) Discrete carboxyl-terminal segments of apolipoprotein E mediate lipoprotein association and protein oligomerization. *J. Biol. Chem. 268*, 15745–15750.
33. Pillot, T., Goethals, M., Najib, J., Labeur, C., Lins, L., Chambaz, J., Brasseur, R., Vandekerckhove, J., and Rosseneu, M. (1999) β-Amyloid peptide interacts specifically with the carboxy-terminal domain of human apolipoprotein E: Relevance to Alzheimer's disease. *J. Neurochem. 72*, 230–237.
34. Aleshkov, S. B., Li, X., Lavrentiadou, S. N., and Zannis, V. I. (1999) Contribution of cysteine 158, the glycosylation site threonine 194, the amino- and carboxy-terminal domains of apolipoprotein E in the binding to amyloid peptide β (1–40). *Biochemistry 38*, 8918–8925.
35. Lins, L., Thomas-Soumarmon, A., Pillot, T., Vandekerchkhove, J., Rosseneu, M., and Brasseur, R. (1999) Molecular determinants of the interaction between the C-terminal domain of Alzheimer's β-amyloid peptide and apolipoprotein E α-helices. *J. Neurochem. 73*, 758–769.
36. Phu, M. J., Hawbecker, S. K., and Narayanaswami, V. (2005) Fluorescence resonance energy transfer analysis of apolipoprotein E C-terminal domain and amyloid β peptide (1–42) interaction. *J. Neurosci. Res. 80*, 877–886.
37. Phillips, J. C., Wriggers, W., Li, Z., Jonas, A., and Schulten, K. (1997) Predicting the structure of apolipoprotein A-I in reconstituted high-density lipoprotein disks. *Biophys. J. 73*, 2337–2346.
38. Weers, P. M., van der Horst, D. J., and Ryan, R. O. (2000) Interaction of locust apolipophorin III with lipoproteins and phospholipid vesicles: Effect of glycosylation. *J. Lipid Res. 41*, 416–423.
39. Fisher, C. A., Narayanaswami, V., and Ryan, R. O. (2000) The lipid-associated conformation of the low density lipoprotein receptor binding domain of human apolipoprotein E. *J. Biol. Chem. 275*, 33601–33606.
40. Lu, B., Morrow, J. A., and Weisgraber, K. H. (2000) Conformational reorganization of the four-helix bundle of human apolipoprotein E in binding to phospholipid. *J. Biol. Chem. 275*, 20775–20781.
41. Narayanaswami, V., Maiorano, J. N., Dhanasekaran, P., Ryan, R. O., Phillips, M. C., Lund-Katz, S., and Davidson, W. S. (2004) Helix orientation of the functional domains in apolipoprotein E in discoidal high density lipoprotein particles. *J. Biol. Chem. 279*, 14273–14279.
42. Drury, J., and Narayanaswami, V. (2005) Examination of lipid-bound conformation of apolipoprotein E4 by pyrene excimer fluorescence. *J. Biol. Chem. 280*, 14605–14610.
43. Vedhachalam, C., Narayanaswami, V., Neto, N., Forte, T. M., Phillips, M. C., Lund-Katz, S., and Bielicki, J. K. (2007) The C-terminal lipid-binding domain of apolipoprotein E is a highly efficient mediator of ABCA1-dependent cholesterol efflux that promotes the assembly of high-density lipoproteins. *Biochemistry 46*, 2583–2593.
44. Hatters, D. M., Peters-Libeu, C. A., and Weisgraber, K. H. (2006) Apolipoprotein E structure: Insights into function. *Trends Biochem. Sci. 31*, 445–454.
45. Narayanaswami, V., and Ryan, R. O. (2000) Molecular basis of exchangeable apolipoprotein function. *Biochim. Biophys. Acta 1483*, 15–36.
46. Saito, H., Dhanasekaran, P., Baldwin, F., Weisgraber, K. H., Lund-Katz, S., and Phillips, M. C. (2001) Lipid binding-induced conformational change in human apolipoprotein E. Evidence for two lipid-bound states on spherical particles. *J. Biol. Chem. 276*, 40949–40954.
47. Aizawa, Y., Fukatsu, R., Takamaru, Y., Tsuzuki, K., Chiba, H., Kobayashi, K., Fujii, N., and Takahata, N. (1997) Amino-terminus truncated apolipoprotein E is the major species in amyloid deposits in Alzheimer's disease-affected brains: A possible role for apolipoprotein E in Alzheimer's disease. *Brain Res. 768*, 208–214.
48. Lambert, M. P., Barlow, A. K., Chromy, B. A., Edwards, C., Freed, R., Liosatos, M., Morgan, T. E., Rozovsky, I., Trommer, B., Viola, K. L., Wals, P., Zhang, C., Finch, C. E., Krafft, G. A., and Klein, W. L. (1998) Diffusible, nonfibrillar ligands derived from Aβ1–42 are potent central nervous system neurotoxins. *Proc. Natl. Acad. Sci. U.S.A. 95*, 6448–6453.
49. Walsh, D. M., Tseng, B. P., Rydel, R. E., Podlisny, M. B., and Selkoe, D. J. (2000) The oligomerization of amyloid β-protein begins intracellularly in cells derived from human brain. *Biochemistry 39*, 10831–10839.
50. Roher, A. E., Chaney, M. O., Kuo, Y. M., Webster, S. D., Stine, W. B., Haverkamp, L. J., Woods, A. S., Cotter, R. J., Tuohy, J. M., Krafft, G. A., Bonnell, B. S., and Emmerling, M. R. (1996) Morphology and toxicity of Aβ-(1–42) dimer derived from neuritic and vascular amyloid deposits of Alzheimer's disease. *J. Biol. Chem. 271*, 20631–20635.
51. Cleary, J. P., Walsh, D. M., Hofmeister, J. J., Shankar, G. M., Kuskowski, M. A., Selkoe, D. J., and Ashe, K. H. (2005) Natural oligomers of the amyloid-β protein specifically disrupt cognitive function. *Nat. Neurosci. 8*, 79–84.
52. Dong, L. M., and Weisgraber, K. H. (1996) Human apolipoprotein E4 domain interaction. Arginine 61 and glutamic acid 255 interact to direct the preference for very low density lipoproteins. *J. Biol. Chem. 271*, 19053–19057.
53. Hatters, D. M., Peters-Libeu, C. A., and Weisgraber, K. H. (2005) Engineering conformational destabilization into mouse apolipoprotein E. A model for a unique property of human apolipoprotein E4. *J. Biol. Chem. 280*, 26477–26482.
54. Zhang, W. Y., Gaynor, P. M., and Kruth, H. S. (1996) Apolipoprotein E produced by human monocyte-derived macrophages mediates cholesterol efflux that occurs in the absence of added cholesterol acceptors. *J. Biol. Chem. 271*, 28641–28646.
55. Herscovitz, H., Gantz, D., Tercyak, A. M., Zannis, V. I., and Small, D. M. (1992) Expression of human apolipoprotein E but not that of apolipoprotein A-I by mouse C127 cells is associated with increased secretion of lipids in the form of vesicles and discs. *J. Lipid Res. 33*, 791–803.
56. Shimano, H., Fukazawa, C., Shibasaki, Y., Mori, N., Gotoda, T., Harada, K., Shimada, M., Yamada, N., Yazaki, Y., and Takaku, F. (1991) The effect of apo E secretion on lipoprotein uptake in transfected cells. *Biochim. Biophys. Acta 1086*, 245–254.
57. Ito, J., Zhang, L. Y., Asai, M., and Yokoyama, S. (1999) Differential generation of high-density lipoprotein by endogenous and exogenous apolipoproteins in cultured fetal rat astrocytes. *J. Neurochem. 72*, 2362–2369.
58. Dory, L. (1989) Synthesis and secretion of apoE in thioglycolate-elicited mouse peritoneal macrophages: Effect of cholesterol efflux. *J. Lipid Res. 30*, 809–816.
59. Zannis, V. I., McPherson, J., Goldberger, G., Karathanasis, S. K., and Breslow, J. L. (1984) Synthesis, intracellular processing, and signal peptide of human apolipoprotein E. *J. Biol. Chem. 259*, 5495–5499.
60. Fagan, A. M., Holtzman, D. M., Munson, G., Mathur, T., Schneider, D., Chang, L. K., Getz, G. S., Reardon, C. A., Lukens, J., Shah, J. A., and LaDu, M. J. (1999) Unique lipoproteins secreted by primary astrocytes from wild type, apoE (−/−), and human apoE transgenic mice. *J. Biol. Chem. 274*, 30001–30007.
61. Huang, Y., Liu, X. Q., Wyss-Coray, T., Brecht, W. J., Sanan, D. A., and Mahley, R. W. (2001) Apolipoprotein E fragments present in

Alzheimer's disease brains induce neurofibrillary tangle-like intracellular inclusions in neurons. *Proc. Natl. Acad. Sci. U.S.A. 98*, 8838–8843.

62. Cho, H. S., Hyman, B. T., Greenberg, S. M., and Rebeck, G. W. (2001) Quantitation of apoE domains in Alzheimer disease brain suggests a role for apoE in Aβ aggregation. *J. Neuropathol. Exp. Neurol. 60*, 342–349.
63. Marques, M. A., Tolar, M., Harmony, J. A., and Crutcher, K. A. (1996) A thrombin cleavage fragment of apolipoprotein E exhibits isoform-specific neurotoxicity. *NeuroReport 7*, 2529–2532.
64. Tolar, M., Marques, M. A., Harmony, J. A., and Crutcher, K. A. (1997) Neurotoxicity of the 22 kDa thrombin-cleavage fragment of apolipoprotein E and related synthetic peptides is receptor-mediated. *J. Neurosci. 17*, 5678–5686.
65. Wellnitz, S., Friedlein, A., Bonanni, C., Anquez, V., Goepfert, F., Loetscher, H., Adessi, C., and Czech, C. (2005) A 13 kDa carboxy-terminal fragment of ApoE stabilizes Aβ hexamers. *J. Neurochem. 94*, 1351–1360.
66. Golabek, A. A., Soto, C., Vogel, T., and Wisniewski, T. (1996) The interaction between apolipoprotein E and Alzheimer's amyloid β-peptide is dependent on β-peptide conformation. *J. Biol. Chem. 271*, 10602–10606.
67. Golabek, A. A., Kida, E., Walus, M., Perez, C., Wisniewski, T., and Soto, C. (2000) Sodium dodecyl sulfate-resistant complexes of Alzheimer's amyloid β-peptide with the N-terminal, receptor binding domain of apolipoprotein E. *Biophys. J. 79*, 1008–1015.

BI702097S